SOME NUMERICAL SOLUTIONS OF STRESSES IN TWO- AND THREE-LAYERED SYSTEMS

R. J. HANK, *Materials and Tests Engineer* AND F. H. SCRIVNER, *Senior Research Engineer, Texas Highway Department*

SYNOPSIS

From Burmister's theory of stress in elastic, layered systems, equations for stress are developed for a point at the first interface on the axis of a circular loaded area. Numerical results are given for various degrees of relative stiffness of the layers comprising two- and three-layered systems.

The case of the frictionless interface in two-layered systems, and the case of perfect continuity at the interface in some typical two- and three-layered sytems, are treated.

Laboratory measured strengths of three soil-cement mixes and two flexible base materials are compared with stress computed from the two-layer theory for a typical condition of loading, and the corresponding required depths of base are arrived at by a graphical method based on the use of the Mohr's rupture envelope.

The three-layer theory is employed to study the effect of thin sub-bases under concrete slabs.

It is concluded that further computations from the theory should be made in conjunction with experimental work directed toward the measurement of stresses in layered systems, and the development of more accurate methods of testing our materials in tension.

In 1943, Professor Donald M. Burmister (*1*)[1] of Columbia University published the general equations for stress in a two-layered system, from the theory of elasticity, for the two conditions:

(1) Perfect continuity at the interface between the two layers, and

(2) No friction at the interface.

The upper layer was assumed to be infinite in extent horizontally but of finite thickness. The lower layer was infinite horizontally and downward.

Later, in 1945, Burmister extended his theory to include a three-layered system with perfect continuity at both interfaces (*3*).

Professor Burmister's general equations can be used directly to determine the stress and displacement anywhere within the layered systems when the surface loading is expressed by the equations:

Vertical stress at surface $= -m\,J_0(mr)$

Shear stress in surface $= 0$.

(r is measured horizontally from the vertical axis of symmetry of the load; m is a parameter inherent in Burmister's solution; $J_0(mr)$ is the symbol for a Bessel's function, similar in some respects to the better known circular functions.)

By performing certain operations on the general equations, involving a triple integration, it is possible to derive the equations for stress and displacement at any point on the vertical axis of a circular area acted on by a surface loading expressed by the equations:

Vertical stress on circular area at surface $= P$

Shear stress in surface $= 0$

where P is constant.

For our purpose (the comparison of computed stress with laboratory measured strength) it appeared that the stresses developed at the interface would be of most interest.[2] Points A and B of Figures 1 and 2 are

[1] Italicized figures in parentheses refer to the list of references at the end of the paper.

[2] Dr. A. Casagrande, in commenting on Burmister's equations, states: ". . . the writer does believe that this approach deserves the attention of all engineers who are conducting research on the design of pavements, and strongly recommends that additional numerical solutions should be prepared as a basis for further studies which are necessary for a safe application of this method (*1*)." Prof. D. W. Taylor states: "There is the possibility that applications of concepts from Burmister's elastic, layered system may be of interest in connection with the Airport base-course problem which is a layered system. However, the stress distributions at the layer boundaries, which are the results that would be of most interest, require extensive computations and have not yet been obtained (*4*)."

the points where stresses were determined. Figures 1 and 2 also show the meaning of the parameters entering into the equations.

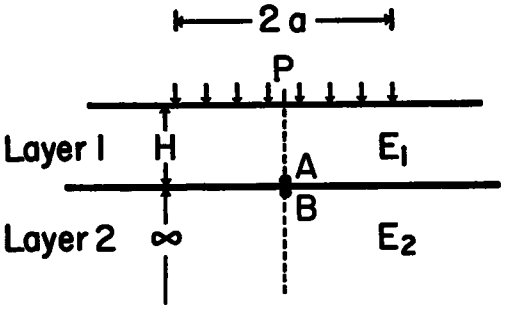

Figure 1. Parameters for Two-Layered System. Stress was computed at points A and B.

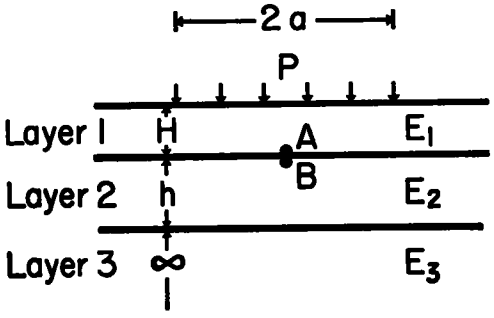

Figure 2. Parameters for Three-Layered System. Stress was computed at points A and B.

TWO-LAYERED SYSTEM

The stress equations used for two-layered systems (detailed derivation shown in appendix) were as follows:

Meaning of Symbols:

E_1 = Youngs modulus of upper layer (layer 1)

E_2 = Youngs modulus of lower layer (layer 2)

$$N = \frac{E_1 - E_2}{E_1 + E_2}$$

$$F = 1/2\left(1 + \frac{E_2}{E_1}\right)$$

a = Radius of circular loaded area.
H = Depth of layer 1.
R = a/H
P = Vertical unit pressure acting on circular area at surface.
m = A parameter inherent in Burmister's solution.
$J_1(mR)$ = Symbol for a Bessel's Function
σr_1 is the radial stress in layer 1,
σr_2 is the radial stress in layer 2.
σz = Vertical stress (same in both layers)
For perfect continuity at interface:

$$\sigma_{r_2} = -\frac{PR(1-N)}{2}\int_0^\infty J_1(mR) \cdot \left[\frac{(2-m)e^m - N(2-5m)e^{-m}}{e^{2m} - 2N(1+2m^2) + N^2e^{-2m}}\right] dm \quad \text{(a)}$$

$$\sigma_z = -PR(1-N)\int_0^\infty J_1(mR) \cdot \left[\frac{(1+m)e^m - N(1-m)e^{-m}}{e^{2m} - 2N(1+2m^2) + N^2e^{-2m}}\right] dm \quad \text{(b)}$$

$$\sigma_{r_1} = \frac{E_1}{E_2}\left[\sigma_{r_2} - \left(1 - \frac{E_2}{E_1}\right)\sigma_z\right] \quad \text{(c)}$$

For frictionless interface:

$$\sigma_{r_1} = PR\int_0^\infty \frac{J_1(mR)\{[(1+F)m + (1-2F)]e^m - [(2-F)m + (1-2F)]e^{-m}\}}{Fe^{2m} + [2(2F-1)m - 1 + 2m^2)] + (1-F)e^{-2m}}\, dm \quad \text{(d)}$$

$$\sigma_{r_2} = \sigma_z = -PR(2F-1)\int_0^\infty \frac{J_1(mR)[(1+m)e^m - (1-m)e^{-m}]}{Fe^{2m} + [2(2F-1)m - (1+2m^2)] + (1-F)e^{-2m}}\, dm \quad \text{(e)}$$

(It will be noted that since these are the stresses at a point on the vertical axis of a symmetrically loaded area, they are principal stresses.)

TABLE 1
INFLUENCE VALUES FOR STRESS AT INTERFACE
(Perfect Continuity at Interface)
(Calculated from Equations (a), (b) and (c))
Tensile Stresses Are Positive
Two-Layered System Flexible Pavement

E_2/E_1	H/a	Vertical	Layer 2 Radial	Layer 1 Radial
.01	1.0	−.0809	−.0449	3.52
	1.111	−.0676	−.0365	3.04
	1.25	−.0552	−.0289	2.57
	1.429	−.0436	−.0222	2.10
	1.667	−.0330	−.0163	1.64
	2.0	−.0237	−.0113	1.22
	2.5	−.0156	−.0072	.82
	3.333	−.0090	−.0040	.49
	5.0	−.0041	−.0018	.23
	10.0	−.0010	−.0004	.06
.05	1.0	−.2047	−.0856	2.178
	1.111	−.1748	−.0698	1.93
	1.25	−.1457	−.0551	1.67
	1.429	−.1177	−.0420	1.40
	1.667	−.0911	−.0306	1.12
	2.0	−.0665	−.0210	.844
	2.5	−.0446	−.0133	.582
	3.333	−.0260	−.0073	.348
	5.0	−.0119	−.0032	.162
	10.0	−.0030	−.0008	.040
0.1	1.0	−.2916	−.1045	1.579
	1.111	−.2523	−.0847	1.424
	1.25	−.2129	−.0667	1.249
	1.429	−.1741	−.0506	1.061
	1.667	−.1364	−.0366	0.862
	2.0	−.1006	−.0248	0.657
	2.5	−.0681	−.0155	0.458
	3.333	−.0401	−.0085	0.276
	5.0	−.0185	−.0037	0.130
	10.0	−.0047	−.0009	0.033
0.3	1.0	−.4629	−.1227	.6710
	1.111	−.4108	−.0986	.6300
	1.25	−.3554	−.0765	.5743
	1.429	−.2976	−.0567	.5053
	1.667	−.2384	−.0397	.4240
	2.0	−.1796	−.0259	.3327
	2.5	−.1236	−.0154	.2370
	3.333	−.0739	−.0081	.1453
	5.0	−.0344	−.0033	.0693
	10.0	−.0088	−.0008	.0180
0.5	1.0	−.5469	−.1230	.3010
	1.111	−.4906	−.0979	.2948
	1.25	−.4297	−.0747	.2802
	1.429	−.3638	−.0542	.2554
	1.667	−.2948	−.0368	.2212
	2.0	−.2240	−.0230	.1780
	2.5	−.1557	−.0129	.1298
	3.333	−.0936	−.0062	.0812
	5.0	−.0439	−.0024	.0392
	10.0	−.0112	−.0006	.0100
1.0[a]	1.00	−.646	−.116	
	1.25	−.524	−.067	
	1.50	−.424	−.040	
	1.75	−.346	−.025	
	2.00	−.284	−.016	
	2.50	−.200	−.008	
	3.00	−.146	−.004	
	4.00	−.087	−.001	
	5.00	−.057	−.001	

[a] Influence values from Table 1 of Ref. 4.

For $E_2 = E_1$, that is, for the homogeneous system treated by Boussinesq, $N = 0$. Substituting $N = 0$ in equations (a), (b) and (c), results in these equations taking the required form for the stress at unit depth on the axis of a circular loaded area.

Dr. L. Fox (7), of the Department of Scientific and Industrial Research, England, whose valuable paper on the two-layered system was published in 1948, has stated in correspondence with the authors that his independent derivation of the above equations agrees with ours.

TABLE 2
INFLUENCE VALUES FOR STRESS AT INTERFACE
(Frictionless Interface)
(Calculated From Equations (d) and (e))
Tensile Stresses Are Positive
Two-Layered System Flexible Pavement

E_2/E_1	H/a	Vertical and Layer 2 Radial	Layer 1 Radial
.1	1.0	−.3050	1.8624
	1.111	−.2633	1.6689
	1.25	−.2221	1.4598
	1.429	−.1813	1.2352
	1.667	−.1420	1.0006
	2.0	−.1046	.7610
	2.5	−.0710	.5290
	3.333	−.0416	.3184
	5.0	−.0191	.1493
	10.0	−.0049	.0381
.3	1.0	−.5030	1.1068
	1.111	−.4444	1.0222
	1.25	−.3833	.9202
	1.429	−.3198	.7993
	1.667	−.2554	.6640
	2.0	−.1916	.5156
	2.5	−.1314	.3650
	3.333	−.0782	.2228
	5.0	−.0363	.1056
	10.0	−.0092	.0271
.5	1.0	−.5979	.8122
	1.111	−.5345	.7630
	1.25	−.4662	.6980
	1.429	−.3933	.6159
	1.667	−.3172	.5181
	2.0	−.2403	.4074
	2.5	−.1663	.2913
	3.333	−.0998	.1793
	5.0	−.0467	.0873
	10.0	−.0119	.0220

The integrals in the above equations were evaluated by approximate methods involving the use of Simpson's rule for approximate integration.

The error involved in the integration is believed to be small (one to two percent).

Table 1 gives influence values for stress for the condition of perfect continuity at the interface: Values of the "stiffness ratio," E_2/E_1, selected were .01, .05, 0.1, 0.3, 0.5, and 1.0.[3]

Table 2 gives influence values for stress for

[3] Values for $E_2/E_1 = 1.0$ taken from tables published in Ref. 5.

TABLE 3
DATA FOR CONSTRUCTION OF MOHR'S CIRCLES OF STRESS
(Perfect Continuity at Interface)
Tensile Stresses are Positive
Two-Layered System Flexible Pavement

E_2/E_1	H/a	Layer 1 Center of Stress Circle	Layer 1 Radius of Stress Circle	Layer 2 Center of Stress Circle	Layer 2 Radius of Stress Circle
.01	1.0	1.720	−1.800	−.0629	−.0180
	1.111	1.485	−1.555	−.0521	−.0156
	1.25	1.260	−1.310	−.0420	−.0132
	1.429	1.030	−1.070	−.0329	− 0107
	1.667	.805	−.835	−.0246	−.0083
	2.0	.600	−.620	−.0175	−.0062
	2.5	.400	−.420	−.0114	−.0042
	3.333	.240	−.250	−.0065	−.0025
	5.0	.115	−.115	−.0030	−.0012
	10.0	.030	−.030	−.0007	−.0003
.05	1.0	.9865	−1.191	−.1451	−.0596
	1.111	.880	−1.050	−.1223	−.0525
	1.25	.762	−.910	−.1004	−.0451
	1.429	.640	−.760	−.0799	−.0379
	1.667	.515	−.605	−.0608	−.0303
	2.0	.388	−.455	−.0437	−.0228
	2.5	.268	− 313	−.0290	−.0157
	3.333	.161	−.187	−.0167	−.0094
	5.0	.075	−.087	−.0075	−.0044
	10.0	.019	−.021	− 0019	−.0011
0.1	1.0	.644	−.935	−.1981	−.0936
	1.111	.586	−.838	−.1685	−.0838
	1.25	.518	−.731	−.1398	−.0731
	1.429	.444	−.618	−.1123	−.0618
	1.667	.363	−.499	−.0865	−.0499
	2.0	.278	− 379	−.0627	−.0379
	2.5	.195	−.263	−.0418	−.0263
	3.333	.118	−.158	−.0243	−.0158
	5.0	.056	−.074	−.0111	−.0074
	10.0	.014	−.019	−.0028	−.0019
0.3	1.0	.1040	−.5670	−.2928	−.1701
	1.111	.1096	−.5204	−.2547	− 1561
	1.25	.1095	−.4648	−.2160	−.1395
	1.429	.1038	−.4015	−.1772	−.1205
	1.667	.0928	−.3312	−.1391	−.0994
	2.0	.0766	−.2562	−.1028	− 0769
	2.5	.0567	−.1803	−.0695	−.0541
	3.333	.0357	−.1096	−.0410	−.0329
	5.0	.0175	−.0518	−.0189	− 0156
	10.0	.0046	−.0134	−.0048	−.0040
0.5	1.0	−.1230	−.4240	−.3350	−.2120
	1.111	−.0979	−.3927	−.2942	−.1964
	1.25	−.0747	−.3550	−.2522	−.1775
	1.429	−.0542	−.3096	−.2090	−.1548
	1.667	−.0368	−.2580	−.1658	−.1290
	2.0	−.0230	−.2010	−.1235	−.1005
	2.5	−.0130	−.1428	−.0843	−.0714
	3.333	−.0062	−.0874	−.0499	−.0437
	5.0	−.0023	−.0416	−.0232	−.0208
	10.0	−.0006	−.0106	−.0059	−.0053

E_2/E_1	H/a	Layers 1 and 2 Center of Stress Circle	Layers 1 and 2 Radius of Stress Circle
1.0	1.0	−.381	−.265
	1.25	−.296	− 228
	1.5	−.232	− 192
	1.75	−.186	−.160
	2.0	−.150	−.134
	2.5	−.104	−.096
	3.0	−.075	−.071
	4.0	−.044	−.043
	5.0	−.029	−.028

$$\text{Center of Stress Circle} = \frac{\sigma z + \sigma r}{2}$$

$$\text{Radius of Stress Circle} = \frac{\sigma z - \sigma r}{2}$$

the condition of a frictionless interface. Values of the "stiffness ratio," E_2/E_1, selected were 0.1, 0.3 and 0.5.

APPLICATION TO FLEXIBLE AND STABILIZED BASES—TWO-LAYER THEORY

There follows a comparison of computed stress with strength as represented by the continuous Mohr's rupture envelope usually

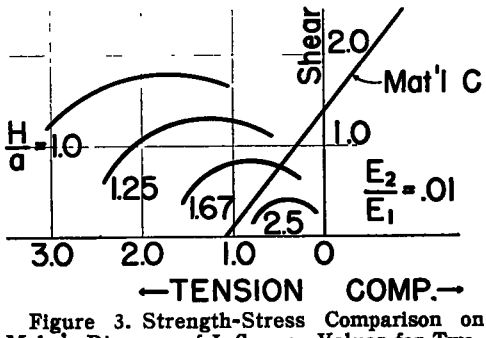

Figure 3. Strength-Stress Comparison on Mohr's Diagram of Influence Values for Two-Layered System. The position of the Layer 1 rupture envelope (the slanting line) depends on cohesion, internal friction and the unit pressure, P, acting on the surface of Layer 1.

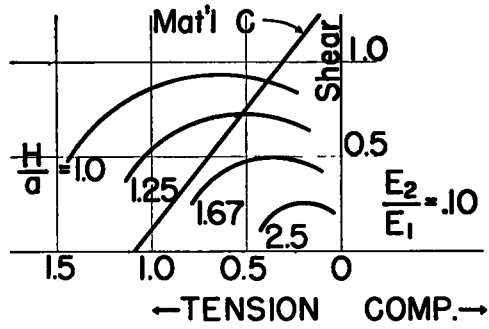

Figure 4. Similar to Fig. 3, but represents a different stiffness ratio. Note that stresses are smaller than those in Fig. 3, showing the effect of a better subgrade.

assumed in theory. In the final step of the comparison, depths of flexible and cement-stabilized bases required on various types of subgrade are computed (see Fig. 6).

Table 3 gives influence values for the computed stresses, for the condition of perfect continuity at the interface, in a form convenient for use in the construction of Mohr's circles of stresses.

Figures 3, 4 and 5 are plots of some of the data given in Table 3 for the upper layer.

Only the useful arcs of the stress circles were drawn in order to avoid confusion, and some circles for which data is presented in Table 3 were omitted for the same reason. Each circle represents the state of stress for a given relative depth, H/a, and a given stiffness ratio, E_2/E_1. Figure 5 shows a comparison between stresses computed from the Burmister and from the better known Boussinesq theory.

Mohr's rupture envelopes, determined from tests in tension and compression, may be plotted on diagrams of the type illustrated by Figures 3, 4 and 5, as follows:

1. From stress-strain curves in compression determine the stiffness ratio, E_2/E_1, for the materials proposed for use as base and subgrade. It is necessary to assume that the modulus in tension equals the modulus in compression for the upper layer.

2. For a given wheel load determine the unit pressure, P, and the radius of contact area, a, to be used in the computations.

3. If σ and τ represent the coordinates of a Mohr's envelope of rupture, then the corresponding coordinates for plotting on Figures 3, 4 or 5 are σ/P and τ/P. If the rupture envelope can be approximated by a straight line, with the equation

$$\tau = C + \sigma \tan \phi$$

where C = cohesion
and ϕ = angle of friction,
then the line may be plotted on diagrams such as Figures 3, 4 and 5 at an inclination of ϕ degrees with the horizontal, and through the point C/P on the axis of zero normal stress.

For comparison of computed stress with laboratory measured strengths, the following loading constants were selected for convenience of interpretation:

P = 100 lb. per sq. in.
a = 5 in.

Wheel load = 7,854 lb.

For example, material C, a soil-cement, had a cohesion of 140 lb. per sq. in., a friction angle of 52 deg., and a tensile strength, from a briquette test, of 97.4 lb. per sq. in. (See Table 5). The rupture line, plotted for the loading constants given above, is shown in Figures 3 and 4.

The value of E_1 for material C, determined from triaxial compression tests, was 385,000 lb. per sq. in. Then by direct interpolation between the stress circles shown in Figure 3, the depth of this material required on a subgrade having a value of E_2 of .01 × E_1 = 3,850 lb. per sq. in. may be estimated as 5 × 2.3 = 11.5 in. The principle used is, of course, that computed stress circles which lie below the rupture line represent safe conditions of stress, while any circle which intersects the rupture line represents a state of stress which would cause failure at the interface.

The rupture line for the foregoing material is also shown in Figure 4, where a required depth of 7.9 in. is indicated on a subgrade with a modulus one tenth as great as that of the soil-cement material. The rupture line for a flexible base, material A, is shown in Figure 5.

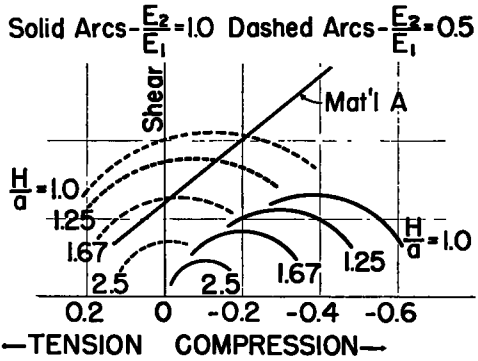

Figure 5. Burmister and Boussinesq Theories Compared. Note that the Boussinesq stresses (the solid arcs) are all compressive. The Burmister stresses are compressive vertically, tensile radially. Material A is a flexible base.

From the data given in Table 3, six influence diagrams of the type shown in Figures 3, 4 and 5 were constructed, and the rupture lines of certain flexible base and cement-stabilized materials, designated as materials A, B, C, D and E in Tables 4 and 5, were plotted on the influence diagrams and required depths of base were obtained by the procedure illustrated above. From the resulting data, which is shown in Tables 4 and 5, the curves in Figure 6 were plotted. Finally, from these curves, the required depth of each material may be determined for any given subgrade modulus, E_2. (The usual range of E_2, from the plastic clays through the stable sand-clays, is from about 2,000 lb. per sq. in. to about 5,000 lb. per sq. in., according to triaxial compression tests made by the Texas Highway Department over the past two years.)

APPLICATION TO CONCRETE PAVEMENT—TWO-LAYER THEORY

In illustrating the application of the Burmister theory to portland cement concrete pavement, it appeared more practical, at this time, to express the strength of the concrete in terms of its flexural (tensile) strength, rather than in terms of its Mohr's envelope of rupture. For this reason, Figures 7, 8 and 9 are plotted in terms of the single stress, σr_1, rather than as Mohr's diagrams similar to those shown in Figures 3, 4 and 5 for flexible materials.

Figure 7 shows the maximum tensile stress in a concrete slab, for an interior load of 10,000 lb. and a load pressure of 100 psi., computed from the two-layer theory. The modulus of the concrete was taken as 4 million psi. (The influence values which furnished the data for plotting the curves in Figure 7 are given in Table 6.)

The stress, of course, varies with the type of subgrade. Curve A gives the stress for a subgrade modulus of 2,000 psi., which, according to our tests, would represent a highly plastic clay. Curve B represents an inferior gravel subgrade, C an excellent gravel subgrade, and D a strongly cemented gravel. The subgrade in each case is assumed to be of infinite depth.

For the great majority of natural subgrades, the stress in the slab, again according to our

TABLE 4
FLEXIBLE BASE MATERIALS

Material	Description	Cohesion	Angle of Friction	Estimated Tensile Strength	Plasticity Index	Thickness, H, required for various values of subgrade modulus (P = 100 psi., a = 5 in.)												
						E_1	E_2/E_1 = .01		E_2/E_1 = .05		E_2/E_1 = .10		E_2/E_1 = .30		E_2/E_1 = .50		E_2/E_1 = 1.00	
							E_2	H	E_2	H	E_2	H	E_2	H	E_2	H	E_2	H
A	Cr. Stone 1½-in. Max. size of aggregate	24.2	39°	23.5	3	17000	170	25	850	21.7	1700	19.2	5100	13.8	8500	10.0	17000	
B	Cr. Stone with cohesionless sand added, 2-in. max. size of aggregate	25.5	48°	20	7	20000	200	30	1000	23.4	2000	21.7	6000	15.0	10000	10.5	20000	

TABLE 5
SOIL-CEMENT MIXTURES

Material	Percent Cement	Cohesion	Angle of Friction	Tensile Strength	Plasticity Index	Thickness, H, required for various values of subgrade modulus (P = 100 psi., a = 5 in.)												
						E_1	E_2/E_1 = .01		E_2/E_1 = .05		E_2/E_1 = .10		E_2/E_1 = .30		E_2/E_1 = .50		E_2/E_1 = 1.00	
							E_2	H	E_2	H	E_2	H	E_2	H	E_2	H	E_2	H
C	8	140	52	97.4	14	385000	3850	11.5	19250	9.4	38500	7.9	115500		192500		385000	
D	8	85	55	51.8	3.5	250000	2500	15.8	12500	13.8	25000	11.5	75000	7.1	125000		250000	
E	8	33	60	16.4	7.7	75000	750	32.5	3750	24.2	7500	22.5	22500	15.4	37500	11.0	75000	

Note: From 97 to 100 percent of all the above samples passed the 40M screen prior to addition of cement.

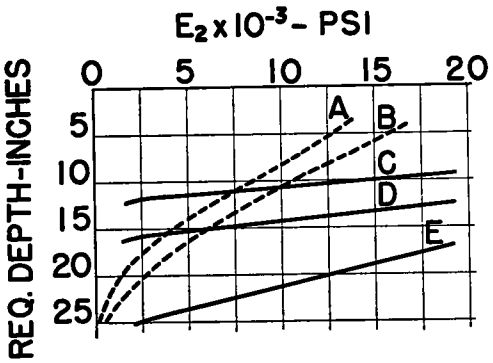

Figure 6. Depth of Base from Two-Layer Theory. A and B are crushed stone; C, D and E are soil-cement materials.

(The influence values which furnished the data for plotting the curves in Figure 7 are given in Table 6.)

The stress, of course, varies with the type of subgrade. Curve A gives the stress for a subgrade modulus of 2,000 psi., which, according to our tests, would represent a highly plastic clay. Curve B represents an inferior gravel subgrade, C an excellent gravel subgrade, and D a strongly cemented gravel. The subgrade in each case is assumed to be of infinite depth.

For the great majority of natural subgrades, the stress in the slab, again according to our

tests, would be represented by points lying in the band between curves A and B. That

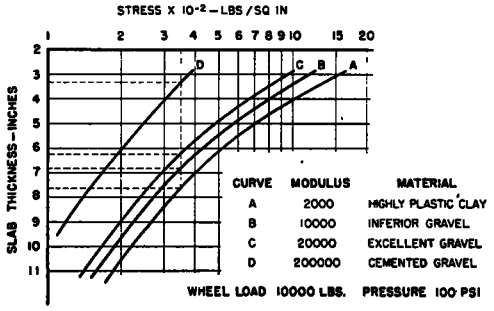

Figure 7. Tensile Stress in Concrete Slab on Various Types of Deep Subgrades. Interior Loading—Two-Layer Systems.

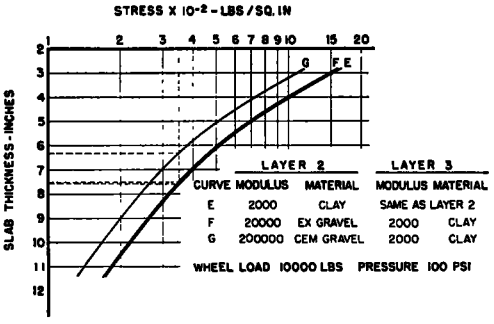

Figure 8. Effect of Thin Sub-bases on A Poor Subgrade. (Thickness of sub-base taken equal to thickness of slab). Tensile Stress in Concrete Pavement, Interior Loading, Two and Three-Layer Systems.

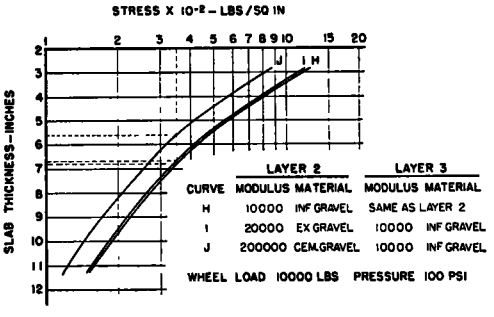

Figure 9. Effect of Thin Sub-bases on An Excellent Subgrade. (Thickness of sub-base taken equal to thickness of slab.) Tensile Stress in Concrete Pavement, Interior Loading—Two and Three-Layer Systems.

is, the points would be between the curves for the highly plastic clay and the inferior gravel.

For a design stress of 350 psi., the depth of the slab, then, would vary from about 6.8 in. to 7.7 in., over the usual range of subgrade types.

What would be the effect on the stress in the slab if a relatively thin sub-base of better material were inserted between the natural soil and the slab? In answering this question we must turn to the three-layer theory.

TABLE 6
INFLUENCE VALUES FOR STRESS AT INTERFACE
(Perfect Continuity at Interface)
(Calculated from Equations (a), (b), and (c))
Tensile Stresses are Positive
Two-Layered System Rigid Pavement

H/a	$E_2/E_1 = 0.0005$			$E_2/E_1 = 0.0025$		
	σ_{r_1}	σ_z	σ_{r_2}	σ_{r_1}	σ_z	σ_{r_2}
0.5000	16.40	−.0437	−.0355	12.45	−.1147	−.0833
1.0000	5.718	−.0121	−.0092	4.706	−.0341	−.0222
1.1111	4.834	−.0099	−.0075	4.010	−.0282	−.0181
1.2500	3.991	−.0079	−.0059	3.337	−.0227	−.0143
1.4286	3.195	−.0061	−.0045	2.694	−.0178	−.0110
1.6667	2.456	−.0046	−.0034	2.087	−.0133	−.0080
2.0000	1.782	−.0032	−.0023	1.526	−.0094	−.0056
2.5000	1.188	−.0021	−.0015	1 024	−.0062	−.0036
3.3333	0.6928	−.0012	− 0009	0.6000	−.0035	−.0020
5.0000	0.3164	−.0005	−.0003	0.2752	−.0016	−.0009
10.0000	0.0805	−.0001	−.0001	0.0702	−.0004	−.0002
H/a	$E_2/E_1 = 0.0050$			$E_2/E_1 = 0.0500$		
	σ_{r_1}	σ_z	σ_{r_2}	σ_{r_1}	σ_z	σ_{r_2}
0.5000	10.08	−.1696	−.1184	3.892	−.4968	−.2774
1.0000	4.069	−.0529	−.0323	2.173	−.2045	−.0856
1.1111	3.494	−.0438	−.0261	1.924	−.1744	−.0695
1.2500	2.929	−.0356	−.0208	1.664	−.1451	−.0546
1.4286	2.380	−.0279	−.0159	1.394	−.1170	−.0414
1.6667	1.850	−.0211	−.0117	1.117	−.0904	−.0300
2.0000	1.358	−.0150	−.0081	0.8424	−.0659	−.0205
2.5000	0.9133	−.0098	−.0052	0.5809	−.0441	−.0128
3.3333	0.5342	−.0056	−.0029	0.3481	−.0258	−.0071
5.0000	0.2459	−.0023	−.0011	0.1623	−.0118	−.0031
10.0000	0.0627	−.0006	−.0003	0.0418	−.0030	−.0008

APPLICATION TO CONCRETE PAVEMENT—THREE-LAYER THEORY

By a process analogous to that used in the two-layer derivations, shown in the appendix, equations similar to equations (a), (b) and (c) have been obtained for the stress at points A and B of Figure 2, for the three-layered system, for several numerical values of the ratio H/h. One set of these equations for $H/h = 1$, is given in the appendix. (Equations (f), (g) and (h).) From these equations the influence values recorded in Table 7, and used in preparing Figures 8 and 9, were computed.

In Figure 8 curve E represents the stress in

a slab resting directly on the clay subgrade (two-layered system). Curve F shows the resulting stress if a gravel subbase, equal in depth to the depth of the concrete slab, is inserted between slab and subgrade (three-layered system). Apparently, the advantage gained in stress reduction is nil. If, however, cement or possibly lime, were added to the gravel, in an amount sufficient to increase its modulus from 20,000 to 200,000 psi., some

TABLE 7
INFLUENCE VALUES FOR STRESS AT FIRST INTERFACE
(Perfect Continuity at Interface)
(Calculated from Equations (f), (g) and (h), for H/h = 1.0)
Tensile Stresses are Positive
Three-Layered System Rigid Pavement

H/a	$E_2/E_1 = 0.0050$ $E_3/E_2 = 0.1000$			$E_2/E_1 = 0.0500$ $E_3/E_2 = 0.0100$		
	σ_{r_1}	σ_z	σ_{r_2}	σ_{r_1}	σ_z	σ_{r_2}
.5000	16.20	−.0599	.0214	11.49	−.1737	.4095
1.0000	5.634	−.0211	.0072	4.197	−.0936	.1209
1.1111	4.760	−.0179	.0060	3.572	−.0828	.0999
1.2500	3.928	−.0148	.0049	2.970	−.0715	.0806
1.4286	3.147	−.0119	.0039	2.397	−.0599	.0629
1.6667	2.419	−.0092	.0029	1.857	−.0479	.0473
2.0000	1.755	−.0067	.0021	1.357	−.0361	.0336
2.5000	1.171	−.0045	.0014	0.9113	−.0249	.0219
3.3333	0.6823	−.0026	.0008	0.5341	−.0149	.0125
5.0000	0.3118	−.0012	.0004	0.2462	−.0069	.0058
10.0000	0.0793	−.0003	.0001	0.0625	−.0018	.0014
H/a	$E_2/E_1 = 0.0050$ $E_3/E_2 = 0.5000$			$E_2/E_1 = 0.0500$ $E_3/E_2 = 0.0500$		
	σ_{r_1}	σ_z	σ_{r_2}	σ_{r_1}	σ_z	σ_{r_2}
.5000	11.87	−.1216	−.0616	8.730	−.2232	.2245
1.0000	4.535	−.0390	−.0161	3.493	−.1069	.0731
1.1111	3.868	−.0325	−.0130	3.000	−.0937	.0610
1.2500	3.225	−.0265	−.0102	2.518	−.0803	.0496
1.4286	2.606	−.0209	−.0078	2.050	−.0666	.0392
1.6667	2.022	−.0159	− 0057	1.602	−.0529	.0298
2.0000	1.480	−.0114	−.0039	1.180	−.0397	.0213
2.5000	.9941	−.0075	−.0025	0.7976	−.0271	.0141
3.3333	.5830	−.0043	−.0014	0.4702	−.0162	.0081
5.0000	.2676	−.0020	−.0007	0.2164	−.0075	.0037
10.0000	.0683	−.0005	−.0002	0.0554	−.0019	.0010

reduction in stress would result, as indicated by curve G. The equivalent saving in slab depth for a design stress of 350 psi. is indicated by the dotted lines.

We have shown here the effect of a relatively thin sub-base built on a poor subgrade. What is the effect if the subgrade is of relatively good quality? The general conclusions are about the same as before, as will be seen from a study of Figure 9.

In Figure 9 the subgrade has a modulus of 10,000 psi., higher than most natural subgrades, according to our tests. Curve H represents the stress when no sub-base is present. Curve I gives the stress if a sub-base of excellent gravel, again equal in depth to that of the concrete slab, is inserted between slab and subgrade. Very little reduction in stress occurs. Curve J represents the case of the stabilized gravel, and once again an appreciable reduction in stress results.

In interpreting the results shown in Figures 8 and 9, it is well to bear in mind that any theoretical analysis is based on the assumption that contact between the slab and the underlying material is maintained at all points and at all times.

CONCLUSIONS

The Burmister theory for layered systems, a solution from the three-dimensional theory of elasticity satisfying the boundary conditions for interior loading, appears to be the most appropriate theory yet proposed for highway and airport design. Considerable labor is involved in the calculation of usable influence values, however, and the work is far from complete. Dr. L. Fox (*7*), whose work was mentioned earlier, will probably publish values for the three-layered system soon, and additional values are being computed by the Texas Highway Department.

Meanwhile, a study of the influence values and graphs presented herein indicates that the experimental work which is necessary to satisfactorily conclude the long and controversial search for a rational design procedure for flexible pavements must include at least the following steps:

1. Development of new testing techniques for the determination of the strengths of our materials under combined (tensile and compressive) states of stress.

The briquette type of test used for testing the soil-cements (materials C, D, and E of Figure 6 and Table 5) may give apparent tensile strengths which are much lower than the true values, according to photo-elastic studies (*6*). The crushed stone materials (A and B) could not be tested in tension with present equipment, and it was necessary to extrapolate the rupture envelopes from the compressive to the tensile side of the Mohr's diagram, a questionable procedure.

2. Measurement of stresses in layered systems.

It may be extremely difficult to measure the tensile stresses which apparently develop at the interface, but it may be possible to measure the vertical compressive stresses with sufficient accuracy using present equipment.

ACKNOWLEDGEMENTS

Aside from personnel of the Texas Highway Department, the authors wish to thank Prof. Raymond F. Dawson and Dr. Dana Young of the University of Texas for their assistance; Prof. Burmister for his review of the paper; and Dr. L. Fox for making available his as yet unpublished equations and influence values for the three-layered system. The receipt of Dr. Fox's equations and numerical results enabled the authors to verify the accuracy of much of the work presented herein.

Within the Department, special thanks are due Chester McDowell, Senior Soils Engineer, and L. E. McCarty, Senior Laboratory Assistant, for their effective help, and to D. C. Greer, State Highway Engineer, under whose supervision the work was done.

REFERENCES

1. D. M. Burmister, "The Theory of Stresses and Displacements in Layered Systems and Applications to the Design of Airport Runways," *Proceedings*, Highway Research Board, Vol. 23, p. 126–148 (1943). See also *Journal of Applied Physics*, Vol. 16, Nos. 2 and 3 (1945).
2. S. Timoshenko, "Theory of Elasticity," McGraw-Hill Book Co., Inc., New York and London, 1934.
3. D. M. Burmister, "The General Theory of Stresses and Displacements in Layered Systems," III, *Journal of Applied Physics*, Vol. 16, p. 296 (1945).
4. Soil Mechanics Fact Finding Survey, Progress Report, Triaxial Shear Research and Pressure Distribution Studies on Soils, Waterways Experiment Station, Vicksburg, Miss., April, 1947, p. 196.
5. E. S. Barber, "Application of Triaxial Compression Test Results to the Calculation of Flexible Pavement Thickness," *Proceedings*, Highway Research Board, Vol. 26, p. 28 (1946).
6. F. O. Anderegg, Royal Weller and B. Fried, "Tension Specimen Shape and Apparent Strength," *Proceedings*, A.S.T.M., Vol. 39, p. 1261 (1939).
7. L. Fox, "Computation of Traffic Stresses in a Simple Road Structure," *Proceedings*, Second International Conference on Soil Mechanics and Foundation Engineering, Vol. 2, p. 236–246 (1948).

APPENDIX

Derivation of Equations for Two-Layered System.

Plane *BCEF* (Fig. 10) is the upper surface of the upper layer.

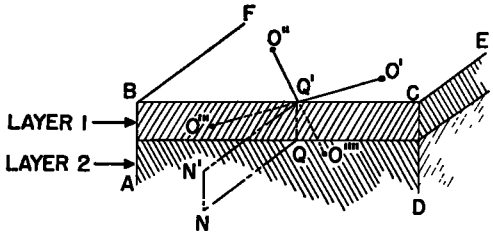

Fig. 10

The vertical axis of any symmetrically distributed stress system passes through the point 0′, an origin of cylindrical coordinates. Point Q is any point at the interface at unit depth. *ABCD* is a given vertical plane through Q, and vertical plane $NN'Q'Q$ is normal to plane *ABCD*.

The stress normal to *ABCD*, at point Q, is from equation (103), p. 183, of Ref. (2):

$$\sigma n' = \sigma r' \cos^2 (N'Q'0') + \sigma_\theta' \sin^2 (N'Q'0') \quad (1)$$

The axis of another equivalent symmetrically distributed stress system is at 0″, such that angle $0'Q'0'' = 90°$. The normal component at Q is

$$\sigma n'' = \sigma r'' \cos^2 (N'Q'0'') + \sigma_\theta'' \sin^2 (N'Q'0'') \quad (2)$$

or

$$\sigma n'' = \sigma r'' \sin^2 (N'Q'0') + \sigma_\theta'' \cos^2 (N'Q'0') \quad (2a)$$

The normal stress at Q due to both loads is

$$\sigma n = \sigma n' + \sigma n'' = \sigma r' \cos^2 (N'Q'0') + \sigma_\theta' \sin^2 (N'Q'0') + \sigma r'' \sin^2 (N'Q'0') + \sigma_\theta'' \cos^2 (N'Q'0') \quad (3)$$

Now let $Q0' = Q0''$
Then $\sigma r' = \sigma r''$
and $\sigma_\theta' = \sigma_\theta''$
From (3):

$$\sigma n = \sigma r' \cos^2 (N'Q'0') + \sigma_\theta' \sin^2 (N'Q'0') + \sigma r' \sin^2 (N'Q'0') + \sigma_\theta' \cos^2 (N'Q'0') \quad (4)$$

Or

$$\sigma n = \sigma r' + \sigma_\theta' \quad (4a)$$

Now

$$\sigma_r' = \frac{\partial}{\partial z}\left[\mu\nabla^2\phi - \frac{\partial^2\phi}{\partial r^2}\right] \quad (5)$$

$$\sigma_\theta' = \frac{\partial}{\partial z}\left[\mu\nabla^2\phi - \frac{1}{r}\frac{\partial\phi}{\partial r}\right] \quad (6)$$

$$\nabla^2 = \left[\frac{\partial^2}{\partial r^2} + \frac{1}{r}\frac{\partial}{\partial r}\frac{\partial^2}{\partial z^2}\right] \quad (7)$$

(See, for instance, page 309, ref. 2).
Let $\mu = \frac{1}{2}$
Then, from (4a) (5) and (6)

$$\sigma n = \frac{\partial^3\phi}{\partial z^3} \quad (8)$$

Now let Q be origin of cylindrical coordinates, r, α, z. The expression for σn is not affected by this change of origin.
From equation (e) of ref. 1:

$$\phi = J_0(mr)[Ae^{mz} - Be^{-mz} + Cze^{mz} - Dze^{-mz}] \quad (9)$$

Then, from (8) and (9)

$$\sigma n = J_0(mr)[m^2e^{mz}(Am + 3C) + m^2e^{-mz}(Bm - 3D) + Cm^3ze^{mz} + Dm^3ze^{-mz}] \quad (10)$$

and the loads acting at 0′ and 0″ are symmetrically distributed about those points at the surface according to the equation, $\sigma z = -mJ_0(mr)$. (See ref. 1.)
At the interface ($z = 0$), from (10),

$$\sigma n = J_0(mr)[m^2(Am + 3C) + m^2(Bm - 3D)] \quad (11)$$

A. For Perfect Continuity at Interface:
From Journal of Applied Physics (Feb. 1945):

$$A_1 = \frac{N}{m^2\Delta}[-(1+m)e^m + N(1-m)e^{-m}]$$

$$B_1 = \frac{1}{m^2\Delta}[(1+m)e^m - N(1-m)e^{-m}]$$

$$C_1 = \frac{N}{m\Delta}[(1+2m)e^m - Ne^{-m}] \quad (A)$$

$$D_1 = \frac{1}{m\Delta}[e^m - N(1-2m)e^{-m}]$$

$$A_2 = C_2 = 0$$

$$\Delta = e^{2m} - 2N(1+2m^2) + N^2e^{-2m}$$

$$N = \frac{E_1 - E_2}{E_1 + E_2}$$

For layer 2 at the interface:

$$\sigma n_2 = mJ_0(mr)[B_2m^2 - 3D_2m] \quad (12)$$

From boundary conditions at the interface, and equations (f) of ref. 1:

$$A_1 + B_1 = B_2 \quad (13)$$

$$A_1m^2 - B_1m^2 + C_1m + D_1m = -B_2m^2 + D_2m \quad (14)$$

From (13) and (14), the left sides of which are known,

$$B_2 = \frac{(1-N)}{m^2\Delta}[(1+m)e^m - N(1-m)e^{-m}] \quad (15)$$

$$D_2 = \frac{(1-N)}{m\Delta}[e^m - N(1-2m)e^{-m}] \quad (16)$$

Finally, from (12), (15) and (16)

$$\sigma n_2 = -mJ_0(mr)(1-N) \cdot \left[\frac{(2-m)e^m - N(2-5m)e^{-m}}{e^{2m} - 2N(1+2m^2) + N^2e^{-2m}}\right] \quad (17)$$

Let σn_F = stress normal to AB at Q due to point loads, F, acting at 0′, 0″, 0‴, 0⁗, all equidistant from Q.
Then

$$\sigma n_F = \frac{F}{2\pi}\int_0^\infty (2\sigma n)\,dm = \frac{F}{\pi}\int_0^\infty \sigma n\,dm \quad (18)$$

(See ref. 1 for an explanation of the general principle involved.)
Let

$$F = Prdrd\,\alpha \quad (19)$$

where P is the uniform vertical pressure distributed at the surface over a circular area, center located directly above point Q, radius

R, this area to include points 0′, 0″, 0‴ and 0⁗,

Let σr_p = radial normal stress at Q, due to the loaded circular area.

From (18) and (19)

$$d\sigma r_P = \frac{P r\, dr\, d\alpha}{\pi} \int_0^\infty \sigma n\, dm \tag{20}$$

and

$$\sigma r_P = \frac{P}{\pi} \int_0^R \int_0^{\pi/2} \int_0^\infty \sigma n\, r\, dr\, d\alpha\, dm \tag{20a}$$

or

$$\sigma r_P = \frac{P}{2} \int_0^R \int_0^\infty \sigma n\, r\, dr\, dm \tag{20b}$$

Substituting (17) in (20b):

$$\sigma r_{P_2} = \frac{-P(1-n)}{2} \int_0^R \int_0^\infty mrJ_0(mr) \cdot \left[\frac{(2-m)e^m - N(2-5m)e^{-m}}{e^{2m} - 2N(1+2m^2) + N^2 e^{-2m}}\right] dr\, dm \tag{21}$$

The integration with respect to r may be performed analytically. Then equation (21) takes the form of equation (a) on page 458.

Vertical Stress

Let σz = vertical stress at Q, due to the load, $-mJ_0(mr)$ with axis of symmetry at 0′.

Let σz_F = vertical stress at Q, due to a point load, F, acting at 0′.

$$\sigma z_F = \frac{F}{2\pi} \int_0^\infty \sigma z\, dm \tag{22}$$

(See ref. 1 for the general principle involved.)

Let $F = Prdrd\ \alpha$ (23)

From (22) and (23):

$$d\sigma z_P = \frac{P r\, dr\, d\alpha}{2\pi} \int_0^\infty \sigma z\, dm \tag{24}$$

Then

$$\sigma z_P = \frac{P}{2\pi} \int_0^R \int_0^{2\pi} \int_0^\infty \sigma z r\, dr\, d\alpha\, dm \tag{24a}$$

Or

$$\sigma z_P = P \int_0^R \int_0^\infty \sigma z r\, dr\, dm \tag{24b}$$

Substituting the value of σz from ref. (1) in (24b)

$$\sigma z_P = -P(1-N) \int_0^R \int_0^\infty mrJ_0(mr) \cdot \left[\frac{(1+m)e^m - N(1-m)e^{-m}}{e^{2m} - 2N(1+2m^2) + N^2 e^{-2m}}\right] dr\, dm \tag{25}$$

After integrating with respect to r, (25) takes the form of equation (b), page 458.

$$\sigma r_{P_1} = \frac{E_1}{E_2}\left[\sigma r_{P_2} - \left(1 - \frac{E_2}{E_1}\right)\sigma z_P\right] \tag{26}$$

(Derived from Hooke's law for the boundary conditions at the interface.)

(26) is identical with equation (c), page 458.

B. For Frictionless Interface:

Radial Stress

From (11)

$$\sigma n_1 = J_0(mr)[m^2(A_1 m + 3C_1) + m^2(B_1 m - 3D_1)] \tag{27}$$

From Journal of Applied Physics (March 1945)

$$\begin{aligned} A_1 m &= -(1-F)(C_1 + D_1) \\ B_1 m &= F(C_1 + D_1) \\ C_1 m &= 1/\Delta_1[(1 - F + m)e^m \\ &\quad - (1-F)e^{-m}] \\ D_1 m &= 1/\Delta_1[Fe^m - (F-m)e^{-m}] \\ \Delta_1 &= Fe^{2m} + (2F-1)2m - (1+2m^2) \\ &\quad + (1-F)e^{-2m} \\ F &= \tfrac{1}{2}\left(1 + \frac{E_2}{E_1}\right) \end{aligned} \tag{B}$$

Substituting in (27):

$$\sigma n = \frac{2mJ_0(mr)}{\Delta_1}\{[(1+F)m + (1-2F)]e^m - [(2-F)m + (1-2F)]e^{-m}\} \tag{28}$$

Substituting (28) in (20b):

$$\sigma r_{P_1} = P \int_0^R \int_0^\infty \frac{mr_0(mr)J}{Fe^{2m} + [2(2F-1)m - (1+2m^2)] + (1-F)e^{-2m}} \{[(1+F)m + (1-2F)]e^m - [(2-F)m + (1-2F)]e^{-m}\}\, dr\, dm \tag{29}$$

$$\sigma z_P = -P(2F-1)\int_0^R\int_0^\infty mrJ_0(mr)\left[\frac{(1+m)e^m-(1-m)e^{-m}}{Fe^{2m}+2(2F-1)m-(1+2m^2)+(1-F)e^{-2m}}\right]dr\,dm \quad (30)$$

After integrating with respect to r, (29) takes the form of (d) on page 458.

Vertical Stress

Substituting σz from Journal of Applied Physics (March, 1945) in (24b)

After integrating with respect to r.

(30) takes the form of (e) on page 458.

Derivation of Equations for Three-Layered System for $H/h = 1.0$ — First Interface.

By a process similar to that already described for the two-layered system, but using the values of the constants A_1, B_1, C_1 and D_1 supplied by Burmister (3) for the three-layered system, equations for stress at the first interface, on the axis of the circular loaded area (points A and B of Fig. 2) were obtained for the special case when the thickness of layer 1 is equal to the thickness of layer 2. As before, Poissons ratio was taken as 1/2. Equations for a general value of H/h, and for both interfaces, have been derived by Dr. Fox (7), and it is presumed that these more valuable equations will be published soon by Dr. Fox. The following equations are given herewith to support the graphs shown in Figures 8 and 9, and the influence values in Table 7.

$$\sigma z = -(1-K)a\int_0^\infty J_1(am)\frac{f_1(m)}{D(m)}\,dm \quad (f)$$

$$\sigma r_1 = \frac{a}{2}\int_0^\infty J_1(am)\frac{g_1(m)}{D(m)}\,dm \quad (g)$$

$$\sigma r_2 = \frac{E_2}{E_1}\left[\sigma r_1 + \left(1-\frac{E_2}{E_1}\right)\sigma z\right] \quad (h)$$

Where

$$\begin{aligned} f_1(m) = {} & e^{-m}(1+m) - Ke^{-3m}(1-m) - N[e^{-3m}(1 \\ & + 3m + 4m^2) + e^{-5m}(1 - 3m + 4m^2)] \\ & + KN[e^{-3m}(1 - m + 4m^3) + e^{-5m}(1 \\ & + m - 4m^3)] + N^2e^{-7m}(1 - m) \\ & - KN^2e^{-5m}(1 + m) \end{aligned}$$

$$\begin{aligned} g_1(m) = {} & - e^{-m}(2 - m) + K[e^{-m}(2 + 5m) \\ & + e^{-3m}(2 - 5m)] + N[e^{-3m}(2 + 9m \\ & - 4m^2) + e^{-5m}(2 - 9m - 4m^2)] \\ & - KN[e^{-3m}(4 - 2m + 8m^2 - 4m^3) \\ & + e^{-5m}(4 + 2m + 8m^2 + 4m^3)] \\ & - K^2e^{-3m}(2 + m) - N^2e^{-7m}(2 + m) \\ & - K^2N^2e^{-5m}(2 - m) + KN^2[e^{-5m}(2 \\ & + 5m) + e - 7m(2 - 5m)] + K^2N[e^{-3m}(2 \\ & + m + 12m^2 + 20m^3) + e^{-5m}(2 - m \\ & + 12m^2 - 20m^3)] \end{aligned}$$

$$\begin{aligned} D(m) = {} & 1 - Ke^{-2m}(2 + 4m^2) - Ne^{-4m}(2 + 16m^2) \\ & + KN(e^{-2m} + e^{-6m})(2 + 4m^2) + K^2(1 \\ & + N^2)e^{-4m} + N^2e^{-8m} - KN^2e^{-6m}(2 \\ & + 4m^2) - K^2Ne^{-4m}(2 + 16m^4) \end{aligned}$$

Where

$$K = \frac{E_1 - E_2}{E_1 + E_2}, \quad \text{and} \quad N = \frac{E_2 - E_3}{E_2 + E_3}$$

DISCUSSION

PROFESSOR D. P. KRYNINE, *University of California*—The authors state that a suitable triaxial equipment for determining strength of frictional materials subjected simultaneously to tension and compression is needed. If really a new test has to be devised, it hardly will be a variation of the triaxial test in which normal stresses only are applied to the sample. To open a tensile fissure in the sample and compress the rest of it, a moment balanced by a tension-compression couple should be applied to the sample. Of course, eccentrical vertical loading of the sample may originate a moment; but such an arrangement probably will be technically inacceptable.